ISSN : 0974 - 7486 Volume 7 Issue 3

Trade Science Inc.

Materials Science

An Indian Journal

Full Paper

MSAIJ, 7(3), 2011 [177-183]

Friction calibration curves using non-conventional specimens

K.K.Pathak[1]*, Vineeta Gurjar[1], Nilesh Mohan[2], Geeta Agnihotri[2]

[1]Advanced Materials and Processes Research Institute (CSIR), Bhopal - 462026, (INDIA)

[2]Deptt. of Mech.Engg., MANIT, Bhopal - 462007, (INDIA)

E-mail : kkpathak1@rediffmail.com

Received: 29th September, 2010 ; Accepted: 9th October, 2010

ABSTRACT

The main objective of this research is to investigate the possibilities of alternative non-conventional specimens for friction calibration. A series of compression tests were simulated on eight non-standard test specimens using Al-2024 as the experimental material. Based on the deformation study, friction calibration curves for the two eligible specimens are developed.

KEYWORDS

Friction calibration curves;
Deformation;
Ring compression test;
Finite element.

INTRODUCTION

It is well known that friction at the interface of die/workpiece plays an important role in the overall integrity of metal forming processes. Friction affects the deformation, load requirement, product surface quality, internal structure of the product, as well as die wear characteristics. Understanding of the friction phenomenon is, therefore significant for understanding what actually happens at the die/workpiece interface under many different conditions and deformation processes. To date, several methods have been developed for quantitative evaluation of friction at the die/work piece interface. Ring compression test is most popular method to evaluate the coefficient of friction.

Some of the prominent works on friction studies are following:

Sofuoglu et al.[8] developed an alternative method to the ring compression test in order to quantitatively evaluate the coefficient of friction, m, at the die/work piece interface. Hayhurst et al[2] proposed a new technique to calibrate the model, which utilizes two test piece geometries, namely the solid cylindrical compression test piece and the ring compression test piece. Sahin Mumin et al.[7] proposed a new approach to investigate the effect of the surface roughness on the frictional properties for different materials and conditions. Rudkins et al[6] performed experimental investigation of friction under hot forming conditions using the ring compression test. The experiments show how variations in temperature at the interface affected the frictional behaviour. Cecil et al.[1] studied the uses of spike forging test as a means of measurement of friction between the die and the work piece. Sofuoglu et al.[8] investigate the effects of material properties, strain-rate sensitivity, and barreling on the behavior of friction calibration curves. Robinson et al.[5] studied the ring compression test using physical modeling experiments and finite element (FE) simulation. Wang et al.[10] developed a new test to incorporate a smooth increase of wrap angle during deformation, even at high deformation rates. Kakkeri et al[3] analysized the

metal forming processes and found that a realistic frictional condition must be specified at the die/workpiece interface in order to obtain accurate metal flow. Rao et al. (2008) used cylindrical Al–Cu alloy samples with initial aspect ratios of 1.0 and 1.5 between flat platens in lubricated and dry conditions to predict the metal flow. Lubrication minimized the barreling of lateral free surface to large extent. Petersen et al.[4] proposed a major improvement in the ability to simulate processes where low tool-work piece interface stresses may prevail. This was confirmed by experimental and numerical investigations into the upsetting of a semi-tapered specimen between parallel dies. From literature survey it is observed that researchers have made attempts to investigate alternate specimens for friction calibration.

In this study eight specimens of different solid geometries were tried for friction prediction between the platens & billets using computer simulation. Based on the deformation studies, correlations has been made between diameter ratios and friction. Out of eight specimens, two were found to be suitable for friction calibration.

Geometrical and material parameters

In this study eight non-conventional specimens have been used for friction calibration. The nomenclatures of these specimens are given in TABLE 1. The dimensions of the specimens are shown in Figure 1-8.

TABLE 1 : Specimens and FE parameters

S.No.	Nomenclature	No. of Elements	No. of Nodes
1.	Center Intrude I	800	861
2.	Profile Extrude	400	441
3.	Hexagon	2400	2542
4.	Center Extrude	800	861
5.	Profile	400	441
6.	I-Section	300	341
7.	Dumble	200	231
8.	Center Intrude II	800	861

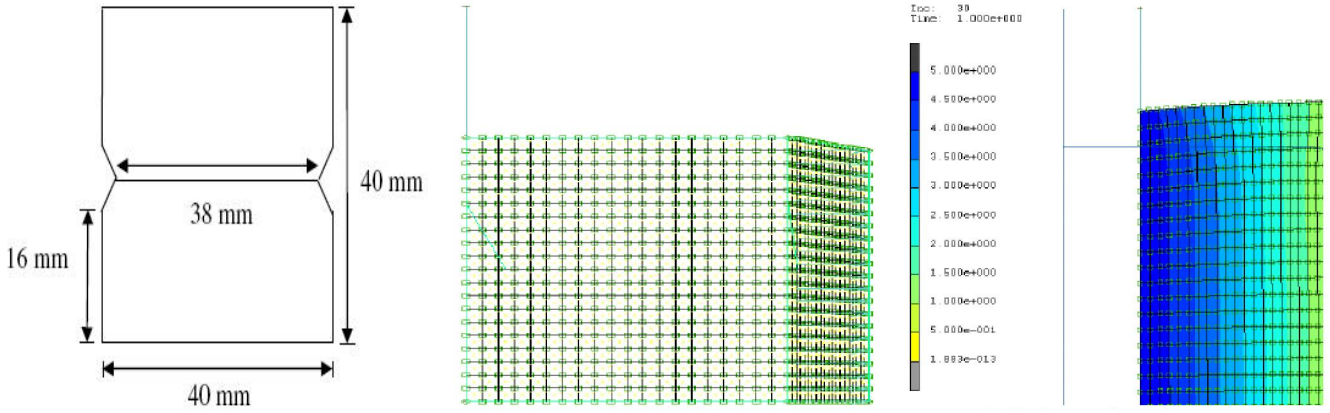

(a) Geometry (b) FE Mesh (c) Deformed mesh

Figure 1 : Geometry and FE model: Center intrude I

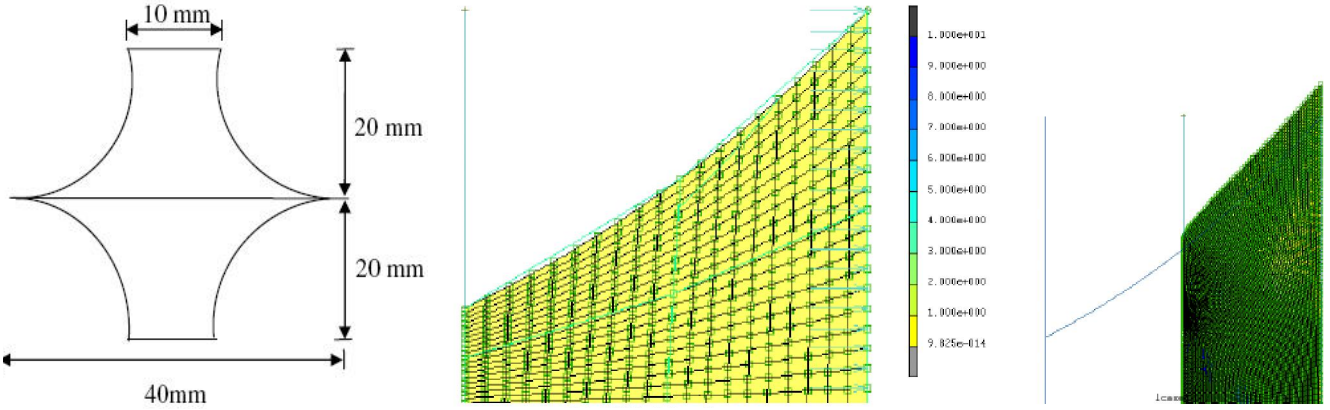

(a) Geometry (b) FE Mesh (c) Deformed mesh

Figure 2 : Geometry and FE model: Profile extrude

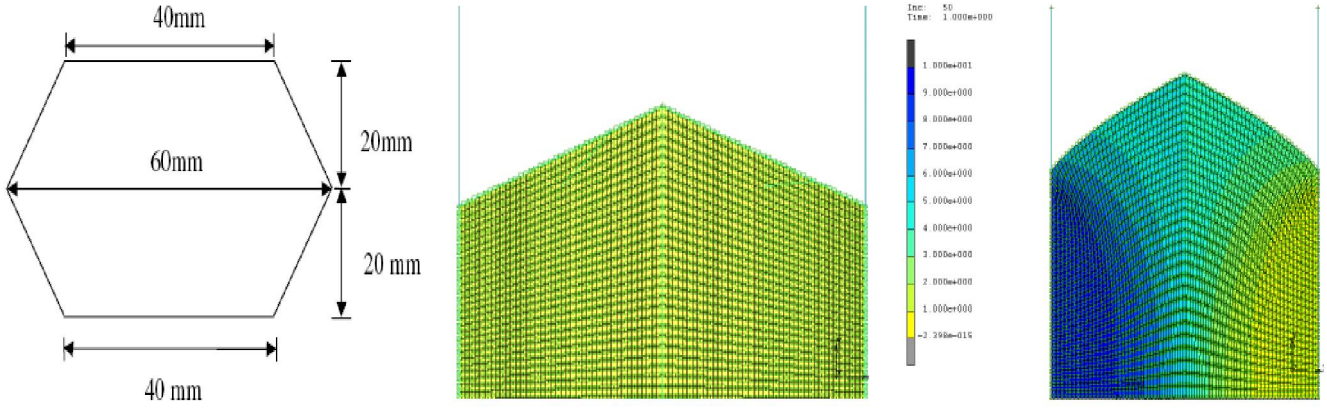

(a) Geometry (b) FE Mesh (c) Deformed mesh

Figure 3 : Geometry & FE model: Hexagon

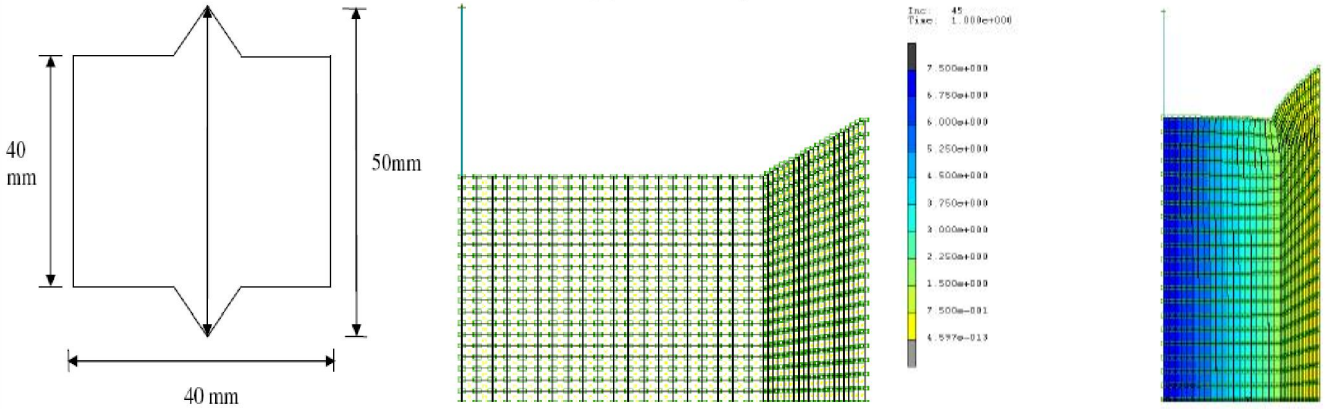

(a) Geometry (b) FE Mesh (c) Deformed mesh

Figure 4 : Geometry & FE model: Center extrude

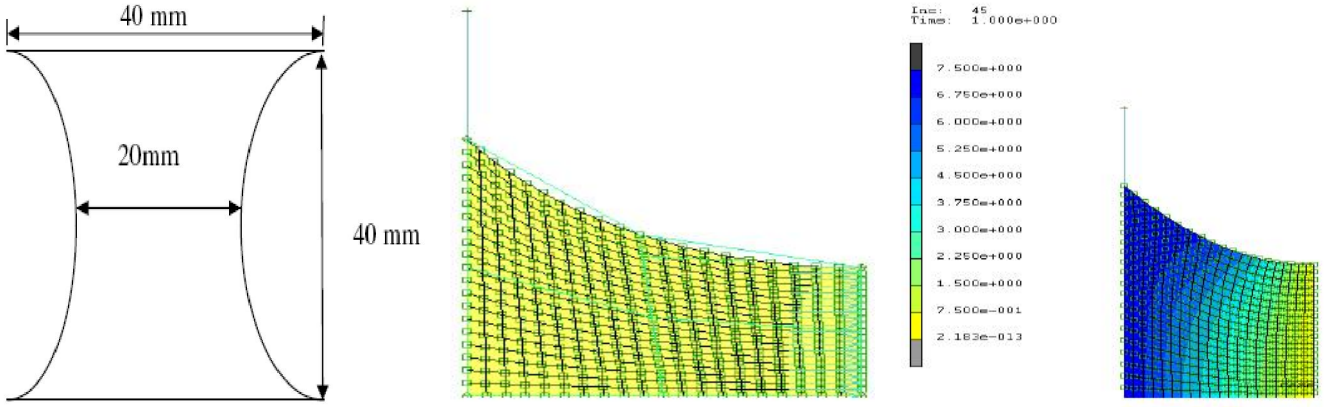

(a) Geometry (b) FE Mesh (c) Deformed mesh

Figure 5 : Geometry & FE model: Profile

Power law, which is given by the following relationship, has been used for material modeling.

$\sigma = k\varepsilon^n$,

Following are the characteristics of the material (Al 2024) taken for numerical experiments:

1. Strength coefficient k = 690 MPa
2. Hardening exponent n = 0.16
3. Young's modulus = 7.8×10^4 N/mm^2
4. Poisson's ratio, $\nu = 0.3$

The coefficient of friction (coulomb) values are taken as 0.1, 0.15, 0.2, 0.25 and 0.3.

FE simulation

Finite element analyses of the compression tests

Full Paper

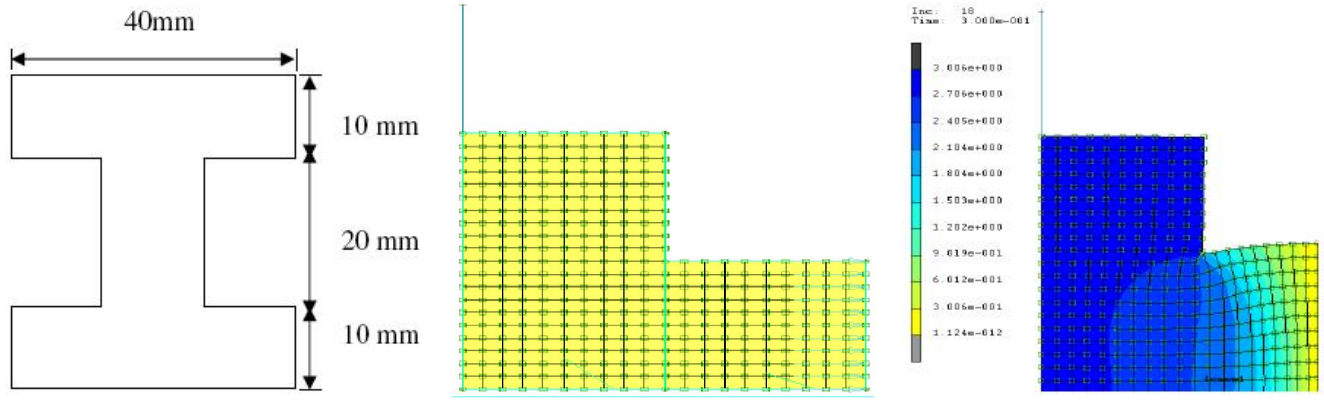

(a) Geometry (b) FE Mesh (c) Deformed mesh

Figure 6 : Geometry & FE model: I-Section

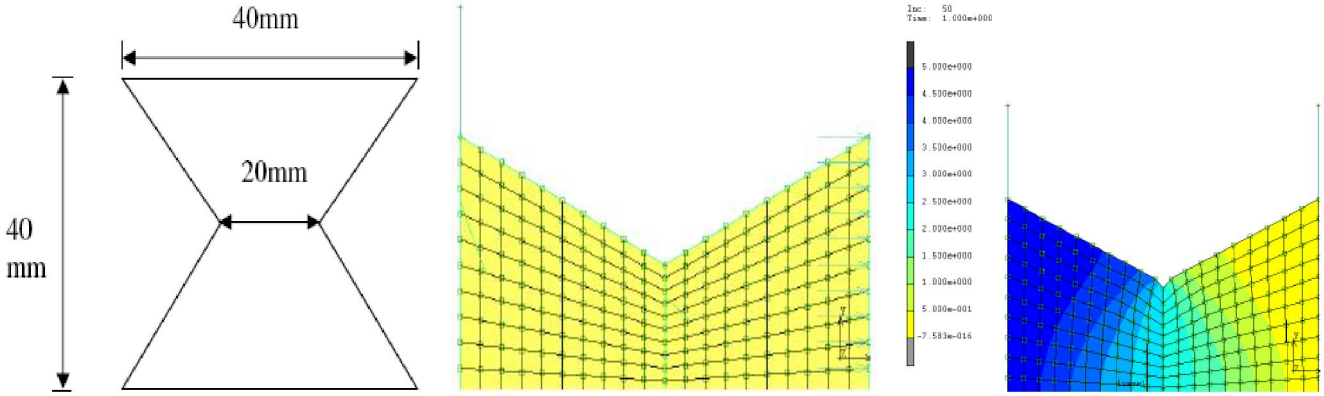

(a) Geometry (b) FE Mesh (c) Deformed mesh

Figure 7 : Geometry & FE model: Dumble

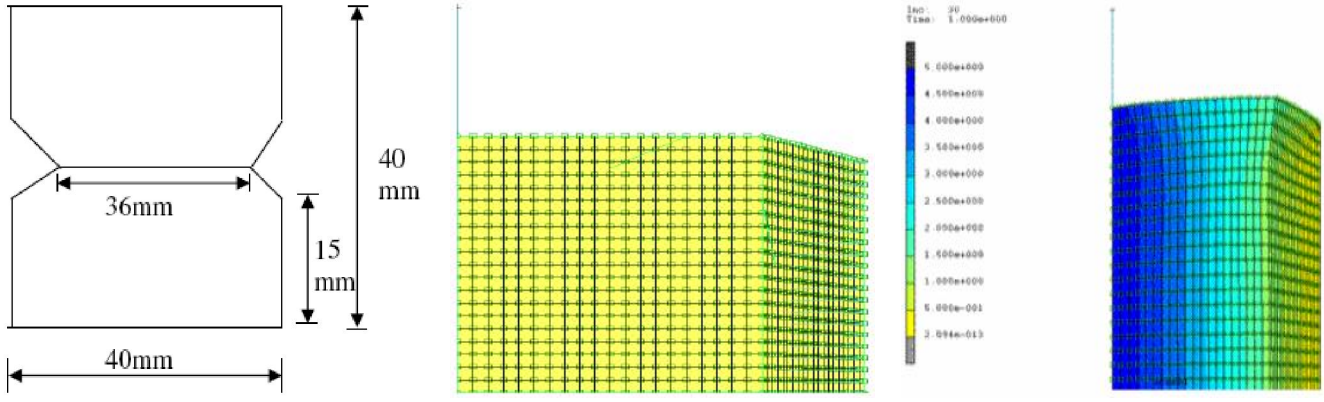

(a) Geometry (b) FE Mesh (c) Deformed mesh

Figure 8 : Geometry & FE model: Center intrude Π

are carried out in order to study the deformation behaviour with respect to friction. Due to symmetric condition only a quarter specimens are modelled. Four noded quadrilateral elements are used for FE modelling. The number of elements and nodes in each model are given in TABLE 1. FE models are shown in Figure 1(b) - 8(b). Specimen is modelled as deformable and platen as rigid bodies. FE simulations are carried out using MSC, MARC software[11]. The interaction of platen and specimen are accounted using CONTACT command. Displacement boundary conditions are applied through the movement of the platen.

RESULTS AND DISCUSSION

A brief summary of the deformation studies of each

specimen is given below:

(a) Center intrude I: The deformed FE mesh is shown in Figure 1(c). The deformed radii at various locations for different friction conditions are recorded and given in TABLE 2. It can be observed, there is continuous increase in left end radius with respect to friction. A calibration curve for 5 mm reduction in height is shown in Figure 9. It can be observed that calibration curve is of linear in nature. The straight line fitting for R^2=0.999 is:

Y=1.763X+21.87

where Y is change in radius and X is the coefficient of friction ranging between 0.1 and 0.3.

TABLE 2 : Deformed radius (mm): Center intrude I

Location	Reduction in height (mm)	Friction				
		0.1	0.15	0.2	0.25	0.3
Left end	2.5	20.3472	20.3831	20.4152	20.448	20.5097
	5	22.0491	22.1403	22.2206	22.3127	22.4037
Right end	2.5	21.1445	21.0497	20.96	20.8728	20.4712
	5	22.5757	22.3372	22.104	21.883	21.6615
Middle end	2.5	21.4101	21.4403	21.4673	21.4945	21.544
	5	23.1922	23.2649	23.3288	23.4023	23.4712

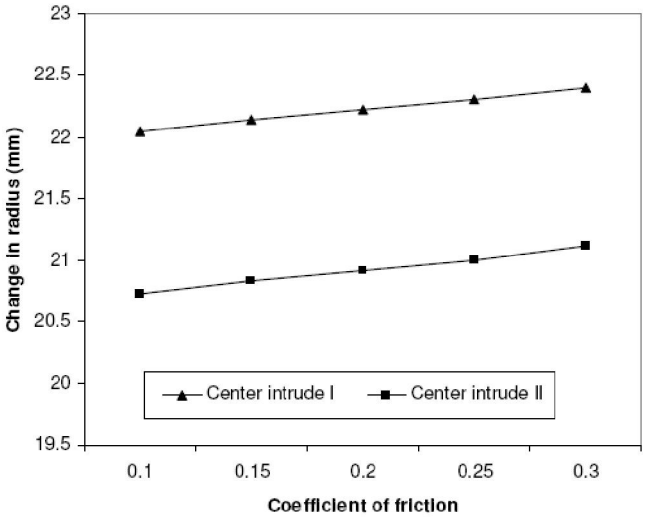

Figure 9 : Friction calibration curve

(b) Profile extrude: The deformed FE mesh is shown in Figure 2(c). The deformed radii at various locations for different friction conditions are recorded and given in TABLE 3. It can be observed, there is not much variation in deformed radii with respect to friction. Hence this specimen is not suitable for generation of friction calibration curve.

(c) Hexagon: The deformed FE mesh is shown in Figure 3(c). The deformed radii at various locations for different friction conditions are recorded and given in TABLE 4. It can be observed, there is not much variation in deformed radii with respect to friction. Hence this specimen is not suitable for generation of friction calibration curve.

TABLE 3 : Deformed radius (mm): Profile extrude

Location	Reduction in height (mm)	Friction			
		0.1	0.15	0.2	0.25
Left end	2.5	6.56372	6.4916	6.4481	6.4294
	5	8.01315	7.9080	7.86717	7.8461
	7.5	9.64592	9.5873	9.57078	9.5519
Right end	2.5	20.0666	20.0617	20.0687	20.0625
	5	20.4257	20.4267	20.4292	20.4362
	7.5	21.1072	21.1082	21.115	21.1141

TABLE 4 : Deformed radius (mm): Hexagon

Location	Reduction in height (mm)	Friction				
		0.1	0.15	0.2	0.25	0.3
Left end	5	26.5724	26.5876	26.5952	26.6015	26.6051
	10	28.4583	28.4806	28.4933	28.5002	28.5089
	15	30.7883	30.8037	30.8148	30.8225	30.8276
	20	33.871	33.8689	33.8632	33.8627	33.8597
Right end	5	20.7434	20.5801	20.3509	20.3938	20.3414
	10	21.9916	22.3049	22.1672	22.0856	21.9829
	15	24.7425	24.461	24.2592	24.0955	23.9543
	20	28.3034	27.6952	27.8154	27.5659	27.4021

(d) Center extrude: The deformed FE mesh is shown in Figure 4(c). The deformed radii at various locations for different friction conditions are recorded and given in TABLE 5. It can be observed, there is not much variation in deformed radii with respect to friction. Hence this specimen is not suitable for generation of friction calibration curve.

TABLE 5 : Deformed radius (mm): Center extrude

Location	Reduction in height (mm)	Friction				
		0.1	0.15	0.2	0.25	0.3
Left end	2.5	26.1716	26.2099	26.2362	26.2539	26.2684
	5	27.3673	27.4534	27.5085	27.5473	27.577
	7.5	28.563	28.669	28.7855	28.8464	28.8925
	10	29.7576	29.9443	30.0643	30.1476	30.2107
Right end	2.5	20.6674	20.562	20.4849	20.4263	20.3824
	5	21.3512	21.1261	20.9693	20.8527	20.7663
	7.5	22.0521	21.7068	21.4688	21.2936	21.1634
	10	22.7666	22.3013	21.9805	21.747	21.5726

Full Paper

(e) Profile: The deformed FE mesh is shown in Figure 5(c). The deformed radii at various locations for different friction conditions are recorded and given in TABLE 6. It can be observed, there is not much variation in deformed radii with respect to friction. Hence this specimen is not suitable for generation of friction calibration curve.

TABLE 6 : Deformed radius (mm): Profile

Location	Reduction in height (mm)	Friction			
		0.1	0.15	0.2	0.25
Left end	2.5	21.0352	20.9986	20.9635	20.9299
	5	2.3809	20.3672	20.3545	20.342
	7.5	22.0243	21.953	21.8821	21.8093
Right end	2.5	12.4794	12.5233	12.5646	12.603
	5	11.2067	11.2202	11.2329	11.2449
	7.5	13.9175	14.0175	14.1104	14.2021

(f) I-section: The deformed FE mesh is shown in Figure 6(c). The deformed radii at various locations for different friction conditions are recorded and given in TABLE 7. It can be observed, there is not much variation in deformed radii with respect to friction. Hence this specimen is not suitable for generation of friction calibration curve.

TABLE 7 : Deformed radius (mm): I-Section

Location	Reduction in height (mm)	Friction				
		0.1	0.15	0.2	0.25	0.3
Left end	2.5	20.0582	20.0573	20.0566	20.0558	20.0551
	5	20.1478	20.1439	20.1403	20.137	20.134
Right end	2.5	11.6172	11.6184	11.6196	11.6207	11.6217
	5	13.1445	13.132	13.1571	13.1626	13.1677

(g) Dumble: The deformed FE mesh is shown in Figure 7(c). The deformed radii at various locations for different friction conditions are recorded and in given TABLE 8. It can be observed, there is not much variation in deformed radii with respect to friction. Hence this specimen is not suitable for generation of friction calibration curve.

TABLE 8 : Deformed radius (mm): Dumble

Location	Reduction in height (mm)	Friction				
		0.1	0.15	0.2	0.25	0.3
Right end	5	31.1611	31.168	31.1729	31.1764	31.179
	10	32.9275	32.9336	32.9404	32.9465	32.9461
	15	35.1934	35.1923	35.1933	35.1918	35.1866
	20	38.3284	38.3805	38.2975	38.2819	38.2675

(h) Center intrude II: The deformed FE mesh is shown in Figure 8(c). The deformed radii at various locations for different friction conditions are recorded and given in TABLE 9. It can be observed, there is continuous increase in left end radius with respect to friction. A calibration curve for 5 mm reduction in height is shown in Figure 9. It can be observed that calibration curve is of linear in nature. The straight line fitting for R^2=0.997 is:

Y=1.9X + 20.536

where Y is change in radius and X is the coefficient of friction ranging between 0.1 and 0.3.

TABLE 9 : Deformed radius (mm): Center intrude Π

Location	Reduction in height (mm)	Friction				
		0.1	0.15	0.2	0.25	0.3
Left end	2.5	21.1322	21.0407	20.9536	20.8727	20.7929
	5	22.5597	22.332	22.107	21.8953	21.6906
Right end	2.5	21.3722	21.4006	21.4262	21.4487	21.4846
	5	23.0924	23.1634	23.2267	23.2827	23.3523
Middle end	2.5	19.8823	19.2664	19.3008	19.331	19.3818
	5	20.72	20.83	20.92	21	21.11

CONCLUSIONS

In this study a search has been made to find alternative specimens for friction calibration using FEM. Total eight non-conventional specimens were tried for this purpose. Out of these eight specimens only two could undergo consistent deformation with respect to varying friction. Friction calibration curves, for these two eligible specimens are generated and found to be of linear in nature where as the conventional ring compression test results in non-linear calibration curves. These non standard specimens can be effectively used as a substitute to ring compression test for friction determination.

REFERENCES

[1] D.M.R.Cecil, A.Rajadurai; Journal of Production Engineering Divisional, The Institution of Engineers (India), **86**, March **(2006)**.

[2] D.R.Hayhurst, M.W.Chan; International Journal of Mechanical Sciences, **47**, 1-25 **(2005)**.

[3] Kakkeri Shrishail, P.Dinesh, Kumar Chetan; International Conference on Advanced Materials and Composites (ICAMC-2007), Oct 24-26, 2007, Organized by National Institute for Interdisciplinary Science & Technology (CSIR), Trivandrum, **(2007)**.

[4] S.B.Petersen, P.A.F.Martins, N.Bay; Journal of Materials Processing Technology, **66**, 186-194 **(1997)**.

[5] T.Robinson, H.Ou, C.G.Armstrong; Journal of Materials Processing Technology, **153-154**, 54-59 **(2004)**.

[6] N.T.Rudkins, P.Hartley, I.Pillinger, D.Petty; Journal of Materials Processing Technology, **60**, 349-353 **(1996)**.

[7] Sahin Mumin, S.C.Cem, Etinarslan, Akata H.Erol; Materials and Design, **28(2)**, 633-640 **(2007)**.

[8] H.Sofuoglu, H.Gedikli; Tribology International, **35**, 27-34 **(2002)**.

[9] Sofuoglu Hasan, Jahan Rasty; Tribology International, **32(6)**, 327-335 **(1999)**.

[10] W.Wang, R.H.Wagoner, X.-J.Wang; Measurement of Friction under Sheet Forming Conditions, **27A**, 3971, December **(1996)**.

[11] User's Manual; MSC, MARC, MSC Software, **(2005)**.